A nonlocal coupled damage-plasticity model for concrete

G.D. Nguyen
Department of Mathematics and Statistics, University of New Mexico (formerly University of Oxford)

A.M. Korsunsky
Department of Engineering Science, University of Oxford

ABSTRACT: The paper presents a non-local constitutive model for the mechanical behaviour of concrete that is based on damage mechanics and plasticity theory. To model the material deterioration due to cracking and residual deformation due to friction, the presented model uses two loading surfaces corresponding to damage and plastic frictional mechanisms. Non-local regularization is used in this study, realized through the non-locality of the energy term in the damage loading function. The particular focus of this study is the calibration of the model parameters. It is shown that both the local behaviour parameters and the parameters governing the non-local material point interaction can be determined from experimental data reliably and consistently. A novel procedure is developed for parameter identification, using the separation of total dissipation energy into additive parts corresponding to different dissipation mechanisms. The relationship between the local and non-local parameters is also addressed, helping to obtain model responses consistent with the fracture energy of the material.

1 INTRODUCTION

Coupled damage-plasticity modelling and non-local regularization have now been widely used for simulating the observed phenomenological behaviour of concrete material, e.g. Yazdani & Schreyer (1990), Luccioni et al. (1996), Lee & Fenves (1998), Meschke et al. (1998), Grassl & Jirásek (2006). The identification and determination of parameters plays an important role in the development of these coupled models, especially for non-local models in which two sets of model parameters control (a) the local behaviour of the model and (b) the spatial interaction of material points. The local set of parameters in this case is related to the behaviour of the model at a pointwise level. On the other hand, the spatial parameter governing the interaction of material points is the length parameter of the non-local continuum and is related to the width of the localization zone. These two sets of parameters are closely related to each other and should be appropriately determined to give the non-local model a response consistent with the required macroscopic material properties. The appearance of the spatial parameter here requires the solution of boundary value problems (BVPs) for the determination of model parameters. This is totally different from a local approach, where the (pointwise) constitutive behaviour of the model can be calibrated directly from experimental data, without the need for solutions of BVPs.

For local coupled damage-plasticity behaviour, the calibration of model parameters so far has not been addressed in detail (e.g. in Meschke et al. 1998, Jefferson 2003), and the choice of model parameters sometimes appears to be rather arbitrary (e.g. in Luccioni et al. 1996), without a clear connection with the experimentally found mechanical properties of the material. From the experimental point of view, Bazant (1996) showed that the fracture energy determined by the work-of-fracture method always contains plastic-frictional dissipation (e.g. due to aggregate interlocking, frictional slips). This conclusion is substantiated by cyclic tests on the tensile-dominant behaviour of concrete (Hordijk 1991, Perdikaris & Romeo, 1995). As a consequence, the energy dissipated per unit volume, represented by the area under the stress-strain curve in continuum models, should be thought to contain contributions from both damage and plasticity mechanisms.

On the other hand, the calibration of parameters for non-local models based on inverse analysis (Carmeliet 1999, Le Bellego et al. 2003) was too complicated and computationally costly to apply widely in practice. Besides, other simple types of calibration based on a linear relationship between the length parameter and the actual width of the localization zone (de Borst & Muhlhaus 1992, Meftah & Reynouard 1998, Di Prisco et al. 2000) could not be considered versatile enough to be applicable for different non-local models with different types of non-local aver-

aging (e.g. non-locality of damage, damage energy or strain) and different softening laws.

The motivation of this study is to develop a non-local coupled damage-plasticity model that would be able to capture essential features of the behaviour of concrete material, with particular focus on the calibration of model parameters. The paper is organized as follows. A coupled damage-plasticity model based on a thermodynamic formulation is briefly outlined in section 2. The model is formulated on the basis of a consistent thermodynamic framework that only requires the specification of two energy functionals and follows procedures established in earlier publications on the subject. Only 2-D behaviour of concrete in tension is considered in this study. The coupling effect between damage and plasticity is briefly outlined in section 2, together with the introduction of non-local behaviour into the model through the appearance of a spatial integral in the damage criterion. In section 3, the calibration of model parameters is presented. Local parameters governing the damage and yielding processes are calibrated based on the damage dissipation and plastic-frictional dissipation, respectively. On the other hand, the link between local and spatial sets of parameters governing the behaviour of the non-local model is also considered to obtain responses of the model consistent with the fracture energy of the material. Numerical examples are presented in section 4 to demonstrate the capability of the proposed constitutive model and the proposed calibration procedures.

2 THERMODYNAMICS-BASED MODELS

2.1 *Formulation*

The formulation for the continuum elasto-plastic-damageable models in this study is based on the thermodynamic framework developed by Houlsby & Puzrin (2000) and modified by Nguyen (2005). A Drucker-Prager type yield criterion is coupled with a damage criterion based on damage energy release rate. The details of this formulation can be found in Nguyen & Korsunsky (2006). For the present it suffices to note that on the basis of this formulation simpler models can be readily worked out where only damage or plastic deformation mechanism operates. The Gibbs free energy function used is

$$g = -\frac{D_{ijkl}\sigma_{ij}\sigma_{kl}}{2(1-\alpha_d)} - \sigma_{ij}\alpha_{ij} \tag{1}$$

with α_{ij} and α_d being the plastic strain tensor and scalar damage variable, respectively, and D_{ijkl} the isotropic elasticity compliance tensor. The dissipation function used takes the following form:

$$d = F_1^*(\alpha_d, \sigma_{ij})\dot{\alpha}_d + k\sqrt{2\dot{\alpha}'_{ij}\dot{\alpha}'_{ij}} + \Lambda_1 C_1 + \Lambda_2 C_2 \tag{2}$$

where α_{ij}' is the deviatoric plastic strain tensor;

$$C_1 = \dot{\alpha}_{kk}/3 - \beta\sqrt{2\dot{\alpha}'_{ij}\dot{\alpha}'_{ij}} = 0 \tag{3}$$

$$C_2 = \dot{\varepsilon}_p - \sqrt{2\dot{\alpha}_{ij}\dot{\alpha}_{ij}/3} = 0 \tag{4}$$

are the two constraints used to define a pressure-dependent yield criterion and the accumulated plastic strain ε_p, respectively, and Λ_1 and Λ_2 are the associated Lagrangian multipliers (Houlsby & Puzrin, 2000); β and k are functions of yield stresses f_{ty} and f_{cy} in tension and compression, respectively:

$$\beta = \frac{f_{cy} - f_{ty}}{\sqrt{3}(f_{cy} + f_{ty})} \text{ and } k = \frac{2 f_{cy} f_{ty}}{\sqrt{3}(f_{cy} + f_{ty})} \tag{5}$$

For coupling behaviour between damage and plasticity, f_{cy} and f_{ty} are expressed as:

$$f_{cy} = (1-\alpha_d)(f'_c + H_t \varepsilon_p) \tag{6}$$

$$f_{ty} = (1-\alpha_d)(f'_t + H_t \varepsilon_p) \tag{7}$$

where $f_c^{'}$ and $f_t^{'}$ are uniaxial strengths in compression and tension, and H_t>0 is the hardening modulus.

The choice of function F_1^* is flexible, provided it is non-negative to assure thermodynamic admissibility of the dissipation process (Nguyen & Korsunsky, 2006). Here the following form is adopted:

$$F_1^*(\alpha_d, \sigma_{ij}) = \begin{cases} 0 & \text{if } \sigma_{ij} = 0 \ (i, j = 1..3) \\ \left[\dfrac{D_{ijkl}\sigma_{ij}\sigma_{kl}}{2(1-\alpha_d)^2}\right]\dfrac{F_1(\alpha_d)}{F_2(\sigma_{ij})} & \text{otherwise} \end{cases} \tag{8}$$

Functions F_1 and F_2 in (8) are defined as follows:

$$F_1(\alpha_d) = \frac{f_t'^2}{2E}\left[\frac{E + E_{pt}(1-\alpha_d)^{n_t}}{E(1-\alpha_d) + E_{pt}(1-\alpha_d)^{n_t}}\right]^2 \tag{9}$$

where E is Young modulus; E_{pt} and n_t are two parameters governing the damage evolution law.

$$F_2(\sigma_{ij}) = \frac{(1+p_t)\sigma_{ij}^+\sigma_{ij}^+ - p_t\langle\sigma_{kk}\rangle\langle\sigma_{ll}\rangle}{2E(1-\alpha_d)^2} \tag{10}$$

where p_t is a parameter controlling the shape of the damage surface in stress space; σ_{ij}^+ is denoted as the positive part of the total stress tensor σ_{ij}, which is decomposed into positive and negative parts using the eigenvalue decomposition (Ortiz 1985).

$$\sigma_{ij}^+ = \sum_{m=1}^{3}\langle\sigma^m\rangle p_i^m p_j^m \tag{11}$$

In the above expression $\mathbf{p}^m$ is the unit vector of the m^{th} principal direction, and σ^m is the m^{th} principal stress.

Following standard procedures established in Houlsby & Puzrin (2000) and illustrated in Nguyen

& Korsunsky (2006), we obtain the constitutive relations governing the behaviour of the model:

$$\varepsilon_{ij} = \frac{D_{ijkl}\sigma_{kl}}{1-\alpha_d} + \alpha_{ij} \tag{12}$$

$$y_p = \beta\sigma_{kk} + \sqrt{\frac{\sigma'_{ij}\sigma'_{ij}}{2}} - k = 0 \tag{13}$$

$$y_d = F_2(\sigma_{ij}) - F_1(\alpha_d) = 0 \tag{14}$$

2.2 *Behaviour of coupled damage-plasticity model*

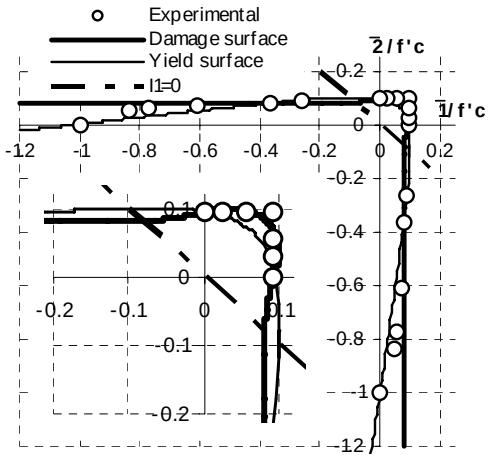

Figure 1. Yield surface and damage failure surface in 2D principal stress space

Figure 1 shows an experimentally determined failure surface (Kupfer & Gerstle 1973), along with numerical yield and damage surfaces in a biaxial test on concrete (I_1 is the first invariant of the stress tensor). In the tension-tension quadrant the yield surface lies inside the damage surface, although the difference between yield and failure surface is small. In other words, plasticity is activated first but only very little plastic strain occurs up to failure. However, both dissipation mechanisms are activated at the same moment in uniaxial tension. Material behaviour beyond peak stress is governed by both damage and plastic deformational mechanisms, which agrees well with experimental observation. In tension-compression regions, tensile damage is the governing dissipation mechanism until the intersection of the yield surface and tensile damage surface is reached, whereupon coupling behaviour occurs. Beyond this intersection point, plasticity is the first dissipation mechanism to take place, followed by coupled damage-plasticity causing the yield surface to expand and reach the failure surface. The contraction of the yield surface in this case is due to the effect of damage, through the progressive reduction of the yield thresholds f_{cy} and f_{ty} (equations 6 & 7) during the fracture process.

2.3 *Non-local regularization*

Non-locality of damage that in concrete can be due to microcrack interactions (Bazant 1991 & 1994). It is implemented in this study through the use of non-local damage energy. The non-local regularization operator L is applied to the energy term $F_2(\sigma_{ij})$ in the damage criterion as follows

$$\tilde{F}_2(\mathbf{x}) = L(F_2(\sigma_{ij})) = \frac{\int_V g(\|\mathbf{y}-\mathbf{x}\|) F_2(\sigma_{ij}(\mathbf{y})) dV_y}{G(\mathbf{x})} \tag{15}$$

where

$$G(\mathbf{x}) = \int_{V_d} g(\|\mathbf{y}-\mathbf{x}\|) dV_y$$

and $g(\|\mathbf{y}\text{-}\mathbf{x}\|)$ is the bell-shaped weight function defined by

$$g(r) = g(\|\mathbf{y}-\mathbf{x}\|) = \begin{cases} 0 & \text{if } r > R \\ \left(1-(r/R)^2\right)^2 & \text{if } r \le R \end{cases} \tag{16}$$

The above weight function depends only on the distance between points within a sphere defined by centre **x** and non-local interaction radius R acting as a length parameter helping to prevent the localization of deformation into an infinitesimally thin zone.

The constitutive behaviour of the model is governed by the following relations: the stress-elastic strain relationship, yield and damage loading function, all of which can be written as:

$$\varepsilon_{ij} = \frac{D_{ijkl}\sigma_{kl}}{1-\alpha_d} + \alpha_{ij} \tag{17}$$

$$y_p = \beta\sigma_{kk} + \sqrt{\frac{\sigma'_{ij}\sigma'_{ij}}{2}} - k = 0 \tag{18}$$

$$y_d = \tilde{F}_2(\mathbf{x}) - F_1(\alpha_d) = 0 \tag{19}$$

The numerical implementation of this model is not presented in this paper, but can be found in Nguyen & Korsunsky (2006), where numerical proof of mesh independence is also illustrated.

3 DETERMINATION OF MODEL PARAMETERS

Calibration of parameters for non-local models has been discussed by several researchers (Bazant & Pijaudier-Cabot 1989, Jirásek 1998, Carmeliet 1999, Le Bellego et al. 2003). Their studies can be generally grouped into two classes: those based directly on numerical inverse analysis of experimental results, and those exploiting the correspondence between the cohesive crack model and the crack band

model. In the first kind of parameter identification (Carmeliet 1999, Le Bellego et al. 2003), automatic calibration of model parameters based on numerical inverse analysis is employed, using optimization algorithms, experimental data from real structural tests and size effect laws. In this method, the length parameter R and other parameters of the local constitutive model are treated equally as general parameters of the non-local constitutive equations in a BVP. However, the complications and expense of solving the inverse problem makes the method difficult to apply widely in practice.

The second kind of parameter identification is pursued in this study, in which the correspondence between the cohesive crack model and crack band model (Bazant 2002, Elices et al. 2002 for details), along with a relationship between the length parameter R of non-local model and the width w_t of the fracture process zone (FPZ), is exploited. This correspondence between cohesive crack model and crack band model has been widely adopted (e.g. in non-local and gradient models used by De Borst & Pamin 1996, Meftah & Reynouard 1998, Jirásek 1998, Di Prisco et al. 2000, Nguyen 2005). Moreover, it is also backed by experimental data for fracture energy, as well as by testing methods to measure the fracture properties of material (e.g. the work of fracture method, size effect method). The displacement jump (or fictitious crack opening) u in the cohesive crack model is smeared out over the crack bandwidth w_t in a continuum model (see Fig. 2 for details). This transforms the experimentally derived stress-separation law in the cohesive crack model into the stress-strain relationship in a continuum model, and helps to determine parameters governing the local constitutive behaviour. This transformation is to give the local constitutive relation a response consistent with the length parameter R, cohesive crack properties (including the fracture energy G_F and the stress-separation curve), and crack bandwidth w_t. The local constitutive behaviour of the model in this case is directly affected by the choice of the length parameter of the model.

In the next section, a procedure for the identification of parameters for local constitutive law is presented, based on the assumption that the imaginary width w_t of the FPZ is known in advance. This is then followed by a procedure for the determination of the relationship between w_t and the non-local interaction radius R. Mutual influences between local and spatial sets of parameters are fully accounted for in the proposed procedure.

3.1 *Parameters governing local constitutive behaviour*

The calibration process is based on the uniaxial tensile test. This approach has been widely accepted and adopted in the research community for its simplicity (e.g. in Meschke et al. 1998, Comi & Perego 2001, Salari et al. 2004). The uniaxial stress-strain curve needed for the determination of model parameters is obtained from the stress-separation law in the cohesive crack model and the width w_t of the FPZ (Fig. 2). The width w_t is defined as that of an imaginary and uniformly damaged crack band and is related to the length parameter of the model.

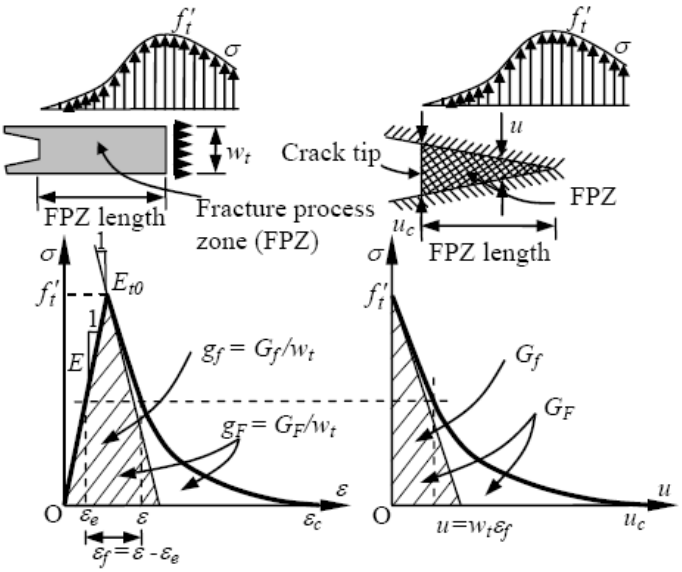

Figure 2. Correspondence between (a) the stress-strain relation in crack band model, and (b) the stress-separation law in cohesive crack model; after Bazant (2002) and Elices et al. (2002)

In the one-dimensional formulation, the energy function and the dissipation function assume the following simplified forms:

$$g = \frac{-\sigma^2}{2E(1-\alpha_d)} - \sigma\alpha_p \tag{20}$$

$$d = F_1(\alpha_d)\dot{\alpha}_d + (1-\alpha_d)(f_t' + H_t\alpha_p)\dot{\alpha}_p \tag{21}$$

where both the plastic strain tensor α_{ij} and the equivalent plastic strain ε_p reduce to α_p such that $\alpha_p \geq 0$ and $d\alpha_p \geq 0$ in uniaxial tension. The local constitutive relations (12-14) now become:

$$\varepsilon = \frac{\sigma}{E(1-\alpha_d)} + \alpha_p \tag{22}$$

$$y_p = \sigma - (1-\alpha_d)(f_t' + H_t\alpha_p) = 0 \tag{23}$$

$$y_d = \frac{\sigma^2}{2E(1-\alpha_d)^2} - F_1(\alpha_d) = 0 \tag{24}$$

where function $F_1(\alpha_d)$ and its two parameters E_{pt} and n_t have been defined in section 2.1. Here it is easier to perform the necessary mathematical manipulations with respect to the damage indicator α_d as the principal variable. Omitting the details of mathematical manipulations we write:

$$\sigma = (1-\alpha_d)\sqrt{2EF_1(\alpha_d)} \tag{25}$$

$$\alpha_p = \frac{1}{H_t}\sqrt{2EF_1(\alpha_d)} - \frac{f_t'}{H_t} \tag{26}$$

$$\varepsilon = \frac{E+H_t}{H_t}\sqrt{\frac{2F_1(\alpha_d)}{E}} - \frac{f_t'}{H_t} \tag{27}$$

The total dissipated energies D_d and D_p due to damage and plasticity, respectively, can be obtained by direct integration of the dissipation rate in equation (21):

$$D_d = \int_0^1 F_1(\alpha_d)\,d\alpha_d \tag{28}$$

$$D_p = \int_0^\infty (1-\alpha_d)\left(f_t' + H_t\alpha_p\right)d\alpha_p \tag{29}$$

The total dissipated energy D is the sum of the energies dissipated due to damage (D_d) and plasticity (D_p). This total dissipated energy is in fact the volumetric fracture energy g_F that can also be obtained as the area under the stress-strain curve, illustrated in Figure 2. Thus:

$$g_F = \int_0^1 F_1(\alpha_d)\,d\alpha_d + \int_0^\infty (1-\alpha_d)\left(f_t' + H_t\alpha_p\right)d\alpha_p \tag{30}$$

The interpretation of experimental results leads to the conclusion that g_F consists of two parts, g_{pF} that is due purely to fracture processes, and (g_F-g_{pF}) that is due to plastic frictional mechanisms (Bazant 1996). This observation is used here for the determination of model parameters. According to Bazant (1996 & 2002), the value of g_{pF} is about 0.2 to 0.5 of g_F, which means that the major part of energy dissipation comes from plastic-frictional mechanisms.

The shape of the stress-separation curve can be used to provide additional input for the calibration process. The experimentally determined fracture energy G_F can be considered to consist of two parts, corresponding to the peak (G_f) and tail (G_F-G_f) responses of the material (Bazant, 2002). By way of interpretation, the area determined from the tangent of the nonlinear stress-strain curve at peak stress (the hatched area in Fig. 2a) is written as g_f=G_f/w_t and taken to be equal to tg_F. For the non-linear softening law in this study, the value of the fraction t lies in the range of 0.1~0.3 and depends on the tensile strength f_t', fracture energy G_F of the material, and the crack bandwidth w_t (Nguyen 2005).

The initial tangent modulus E_{t0} at peak stress (Fig. 2a) is needed to determine the initial volumetric fracture energy g_f. This modulus can be obtained by differentiating (25) and (27) with respect to α_d and substituting α_d=0 into the obtained expression:

$$E_{t0} = -\frac{E_{pt}H_t}{E+H_t} \tag{31}$$

Therefore after substituting (26) and its derivative with respect to α_d into (28-29) we have the following system of equations for the determination of model parameters:

$$g_{pF} = D_d = \frac{f_t'^2}{2E} + \int_0^1 (1-\alpha_d)\frac{\partial F_1}{\partial \alpha_d}\,d\alpha_d \tag{32}$$

$$g_F - g_{pF} = D_p = \frac{E}{H_t}\int_0^1 (1-\alpha_d)\frac{\partial F_1}{\partial \alpha_d}\,d\alpha_d \tag{33}$$

$$g_f = tg_F = \frac{f_t'^2}{2}\left(\frac{1}{E} + \frac{E+H_t}{E_{pt}H_t}\right) \tag{34}$$

The above system of nonlinear equations can be solved numerically using a Matlab code. A simple numerical example is given here to demonstrate the proposed procedure for the parameter identification. The following material properties and parameters were used: Young's modulus E=38000MPa, tensile strength f_t'=3MPa, fracture energy G_F=0.125N/mm, crack bandwidth w_t=20mm, and t=g_f/g_F=0.2.

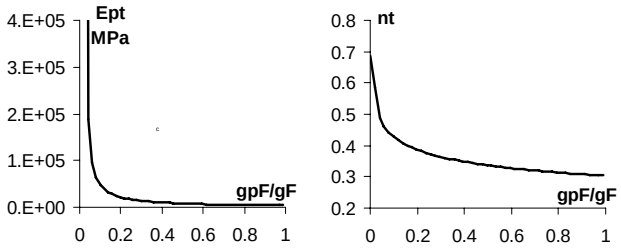

Figure 3. The dependence of damage parameters E_{pt} and n_t on the ratio g_{pF}/g_F

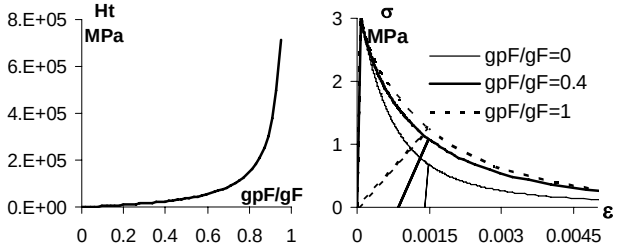

Figure 4. The effect of the ratio g_{pF}/g_F (a) on the hardening modulus H_t, and (b) on the stress-strain behaviour of the model.

The effects of the ratio g_{pF}/g_F on the model parameters and stress-strain behaviour are illustrated in Figures 3-4. Plasticity-dominated response can be obtained by using $g_{pF}/g_F \approx 0$ ($H_t \approx 0$ in this case), while damage-dominated response is recovered by setting g_{pF}/g_F=1 (H_t=$\propto$ in this case). In all cases (Fig. 4b; very long tails are not plotted) the total fracture en-

ergy g_F remained unchanged (see equations 32 & 33). We note that the experimentally observed values of the ratio g_{pF}/g_F between 0.2 and 0.5 (Bazant 1996 & 2002) result in coupled damage-plasticity behaviour (Fig. 4b). It should also be noted here that a perfect case with plasticity being the only dissipation mechanism cannot be derived from the coupled model presented above, as the softening behaviour of the model is mainly governed by damage mechanism. However, a nearly perfect case with $H_t \approx 0$ can be used to derive models with plasticity-dominated responses.

3.2 *Parameter governing the spatial interaction*

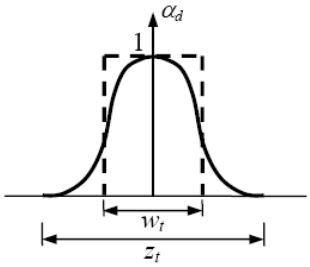

Figure 5. Damage profile in uniaxial test using non-local model, and definition of w_t and z_t (adapted from Bazant & Pijaudier-Cabot 1989)

As can be seen, the parameters governing the local constitutive behaviour of a non-local model are dependent on the imaginary width w_t of the FPZ. In the crack band approach, as strain localizes in one element, w_t must be dependent on the finite element size h to assure the right amount of dissipation specified by the fracture energy G_F (Bazant & Oh, 1983) and the independence from the finite element size of the dissipation per unit advance of the crack band. Nevertheless, the width of the localization zone in non-local analysis, defined by z_t (see Fig. 5), may contain several softened finite elements with different constitutive behaviour due to the non-local averaging process. It is therefore difficult, even impossible, to determine the relationship between w_t and the length parameter R analytically in non-local models, except in some simple cases with a linear softening law (e.g. in De Borst & Muhlhaus 1992, Meftah & Reynouard 1998, Zhao et al. 2005).

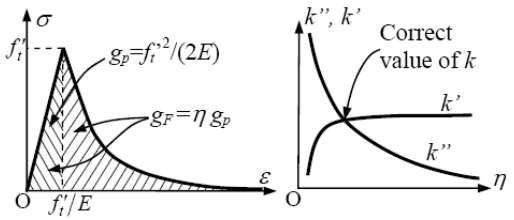

Figure 6. (a) Definition of the ductility parameter η, and (b) determination of the ratio $k=w_t/R$

For that reason, a condition on the equivalence between the energy dissipated by a non-local model with imaginary crack bandwidth w_t and that specified by the fracture energy G_F is used in this study. Non-local numerical analyses of a simple bar under uniaxial tension will be carried out for the determination of a relationship between w_t and the length parameter R of the non-local model.

In the numerical analysis, it is assumed that w_t is proportional to the length parameter R by the ratio $k=w_t/R$. This is practically reasonable, as the dependence of w_t on other parameters of the model is implicitly embedded in the procedure proposed. The relationship between g_F and G_F can be rewritten as

$$G_F = w_t g_F = kRg_F \tag{35}$$

where k is the unknown ratio to be determined. Relationships between non-dimensional quantities are used to make the process of determining the ratio k easier. Jirásek (1998) suggested using the relationships between the ductility parameter η, defined as the ratio of the volumetric fracture energy g_F to the elastic energy density g_p at peak stress (Fig. 6a), and the relative dissipation length as the ratio between w_t and the length parameter of the non-local model. For the use of the bell-shaped function in this study, $k=w_t/R$ is adopted as the relative dissipation length. The proposed procedures can be summarized as follows:

- Assume values of k_i"'s: k_1"=1.0, …, k_n"=3.0 for the coupled model in this study.
- Calculate fracture energies $g_{Fi}=G_F/(Rk_i")$, ductility parameters $\eta_i=g_{Fi}/g_p$ (see Fig. 6a) and determine the corresponding sets of parameters for local damage model, based on eqs. (32-34).
- Carry out the numerical analyses of a one-dimensional bar and calculate the corresponding total dissipated energies D_i as the areas under the load-displacement curves.
- From the obtained dissipated energies, calculate the corresponding fracture energies $G_{Fi}'=D_i/A$, where A is the cross-sectional area of the bar, and derive the ratios $k_i'=G_{Fi}'/(Rg_{Fi})$.
- The correct value of k will be found by plotting $k_i"$ and k_i' against $\eta_i=g_{Fi}/g_p$ and determining the intersection point of the two plotted curves (see Fig. 6b).

A literature review on the determination of the ratio $k=w_t/R$ for non-local models, along with further details on the procedure and corresponding numerical illustrations can be found in Nguyen (2005) and Nguyen & Houlsby (2006).

4 NUMERICAL EXAMPLES

4.1 *Cyclic tension test*

This example was taken from the paper by Lee & Fenves (1998), with corresponding experimental data provided by Gopalaratnam & Shah (1985). The following material properties are used (Gopalarat-

nam and Shah, 1985): E=31700MPa, ν=0.18, f_t'=3.48MPa, G_F=0.04N/mm. The stress-strain curve is obtained from the test by simply dividing the displacement in the stress-displacement curve by the gauge length. This is obviously erroneous as there is no unique stress-strain relationship in the post-peak softening region (Gopalaratnam & Shah 1985). However, it is assumed here just to transform the stress-displacement curve to a stress-strain curve for illustrating the calibration procedure and the capability of the proposed model. In a similar way, the specific fracture energy g_F is calculated by assuming that the localization bandwidth is w_t=45mm, resulting in g_F=0.00089N/mm^2. Obviously this choice of w_t is arbitrary, and is used here only for the purpose of demonstrating the proposed identification procedure. Using the ratios g_f/g_F=0.3 and g_{pF}/g_F=0.26, we obtain the following model parameters, as solutions of system (32-34): E_{pt}=1076700MPa, H_t=1122MPa, n_t=0.52. The stress-strain response is plotted in Figure 7, showing that both the stiffness reduction and permanent deformation are captured well by the model.

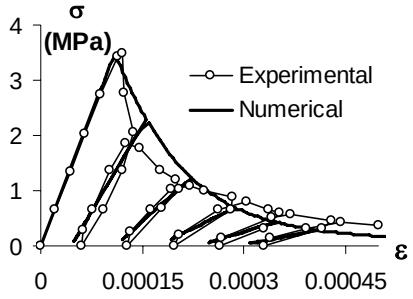

Figure 7. Stress-strain behaviour in cyclic tension test

4.2 *Four-point bending test of a notched beam under cyclic loading*

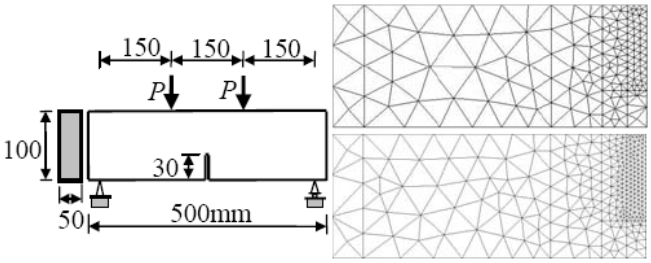

Figure 8. Four-point bending test - Geometry and FE meshes

In this example, the four-point bending test experimentally performed by Hordijk (1991) is simulated using the coupled damage-plasticity model. The geometry of the specimen and FE meshes of a half-beam model are depicted in Figure 8. The following material properties were given: E=38000MPa, ν=0.2, f_t'=3.0MPa, G_F=125N/m, with the assumed ultimate stress in uniaxial compression f_c'=30MPa.

Three different non-local radii (Table 1) were used for the numerical simulations. The ratios t=G_f/G_F=0.2 and G_{pF}/G_F=0.48 were assumed (see section 3). Three parameter sets corresponding to three different non-local radii are obtained using the procedure in section 3, and shown in Table 1.

Table 1. Parameters of local model corresponding to choice of non-local radii

Non-local radius	Model parameters			
	k	H_t (MPa)	E_{pt} (MPa)	n_t
R_1 =12mm	2.05	33371	10738	0.35
R_2 = 9mm	2.14	33745	8098	0.34
R_3 = 6mm	2.32	33800	6381	0.33

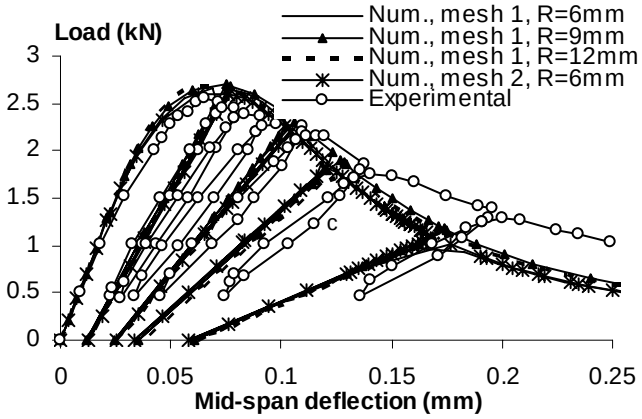

Figure 9. Four-point bending test - Load-deflection curves

The load-deflection curves are shown in Figure 9. It can be seen that all the numerical curves match each other rather well and there is almost no difference in the numerical results using different FE meshes and different non-local radii. This is an important feature showing both the capability of the proposed calibration procedure and the regularization effect of this non-local model. The permanent deformations at zero stress state are clearly seen in Figure 9, showing the capability of the model in capturing residual strains in tension. In addition, due to the fixed ratio G_{pF}/G_F used in the calibration, the parameter H_t is almost invariant (relative change of less than 1.5%) with the change of non-local radius (Table 1), and unloading paths from solutions using different radii almost coincide.

5 CONCLUSIONS

A thermodynamics-based coupled damage-plasticity model has been developed. Coupling between two dissipation mechanisms of isotropic damage and plasticity is fully taken into account in the proposed model. In addition, enhancement to the model to cope with softening-related problems is also made, using non-local energy-based damage criterion. The identification and determination of model parameters have been carefully taken into account during the model development. Relationships between the material properties and model parameters for non-local constitutive models have been established,

helping to identify properly model parameters from experimentally measured properties of the material. Although choice of the best set of parameters, which corresponds to the material characteristic length, can be made on the basis of size effect tests and optimization methods (Carmeliet 1999, Le Bellego et al. 2003), for practical purposes, use of any reliable set of model parameters based on the proposed method is acceptable, as the model responses in this case are consistent with the input fracture energy G_F. Further enhancements to the model are also required, lying in the use of anisotropic damage and plasticity mechanisms and a mechanism to account for the unilateral behaviour of the material.

ACKNOWLEDGEMENTS

Financial support from the Jenks family (in the U.S.A.) through the Peter Jenks Vietnam scholarship to the first author is gratefully acknowledged.

REFERENCES

Bazant, Z.P. 1991. Why continuum damage is nonlocal: Micromechanics arguments. *ASCE Journal of engineering mechanics* 117(5): 1070-1087.

Bazant, Z.P. 1994. Nonlocal damage theory based on micromechanics of crack interactions. *ASCE Journal of engineering mechanics* 120(3): 593-617.

Bazant, Z.P. 1996. Analysis of work-of-fracture method for measuring fracture energy of concrete. *ASCE Journal of engineering mechanics* 122(2): 138-144.

Bazant, Z.P. 2002. Concrete fracture models: testing and practice. *Engineering fracture mechanics* 69: 165-205.

Bazant, Z.P., & Oh, B.H. 1983. Crack band theory for fracture of concrete. *Materials and structures* (RILEM, Paris) 16: 155-177.

Bazant, Z.P., & Pijaudier-Cabot, G. 1989. Measurement of characteristic length of nonlocal continuum. *ASCE Journal of engineering mechanics* 115(4): 755-767.

Carmeliet J. 1999. Optimal estimation of gradient damage parameters from localization phenomena in quasi-brittle materials. *Mechanics of cohesive-frictional materials* 4: 1-16.

Comi, C. & Perego, U. 2001. Fracture energy based bi-dissipative damage model for concrete. *International journal of solids and structures* 38: 6427-6454.

De Borst, R. & Muhlhaus, H-B. 1992. Gradient-dependent plasticity: formulation and Algorithmic aspects. *International journal for numerical methods in engineering* 35: 521-539.

De Borst, R. & Pamin, J. 1996. Gradient plasticity in numerical simulation of concrete cracking. *European journal of mechanics A/Solids* 15(2): 295-320.

Di Prisco, M., Ferrara, L., Meftah, F., Pamin, J., De Borst, R., Mazars, J. & Reynouard, J.M, 2000. Mixed mode fracture in plain and reinforced concrete: some results on benchmark tests. *International journal of fracture* 103: 127-148.

Elices, M., Guinea, G.V., Gomez, J. & Planas, J. 2002. The cohesive zone model: advantages. limitations and challenges, *Engineering fracture mechanics* 69: 137-163.

Gopalaratnam, V.S. & Shah, S.P. 1985. Sofnening response of plain concrete in direct tension. *ACI Materials journal* 82(3): 310-323.

Grassl P. & Jirásek M. 2006. Plastic model with non-local damage applied to concrete. *International journal for numerical and analytical method in geomechanics* 30: 71-90.

Hordijk, D.A. 1991. Local approach to fatigue of concrete, *PhD dissertation*. Delft University of Technology, Delft, The Netherlands.

Houlsby, G.T. & Puzrin, A.M. 2000. A thermomechanical framework for constitutive models for rate-independent dissipative materials. *International journal of plasticity* 16: 1017-1047.

Jefferson, A.D. 2003. Craft – a plastic-damage-contact model for concrete. I. Model theory and thermodynamic considerations. *International journal of solids and structures* 40: 5973-5999.

Jirásek M. 1998. Comparison of non-local models for damage and fracture. *LSC Internal report 98/02*, Department of Civil Engineering, Swiss Federal Institutive of Technology (EPFL), Lausanne, Switzerland.

Kupfer, H.B. & Gerstle, K.H. 1973. Behavior of concrete under biaxial stresses. *ASCE Journal of engineering mechanics* 99(EM4): 853-866.

Le Bellego C., Dube J.F., Pijaudier-Cabot G. & Gerard B. 2003. Calibration of nonlocal damage model from size effect tests. *European journal of mechanics A/Solids* 22: 33-46.

Lee, J. & Fenves, G.L. 1998. A plastic-damage concrete model for earthquake analysis of dams. *Earthquake engineering and structural dynamics* 27: 937-956.

Luccioni, B., Oller, S. & Danesi, R. 1996. Coupled plastic-damaged model. *Computer methods in applied mechanics and engineering* 129: 81-89.

Meftah, F. & Reynouard, J.M. 1998. A multilayered mixed beam element in gradient plasticity for the analysis of localized failure modes. *Mechanics of cohesive-frictional materials* 3: 305-322.

Meschke, G., Lackner, R. & Mang, H.A. 1998. An anisotropic elastoplastic-damage model for plain concrete. *International journal for numerical methods in engineering* 42: 703-727.

Nguyen G.D. & Houlsby G.T. 2006. Non-local damage modelling of concrete: a procedure for the determination of parameters. *International journal for numerical and analytical methods in geomechanics*. in press.

Nguyen, G.D. 2005. A thermodynamic approach to constitutive modelling of concrete using damage mechanics and plasticity theory. *D.Phil. dissertation*. Department of Engineering Science, University of Oxford, UK.

Nguyen, G.D. & Korsunsky, A.M. 2006. Development of a consistent approach to constitutive modelling of concrete using damage mechanics and plasticity theory, to be submitted.

Ortiz, M. 1985. A constitutive theory for the inelastic behavior of concrete. *Mechanics of materials* 4: 67-93.

Perdikaris, P.C. & Romeo, A. 1995. Size effect on fracture energy of concrete and stability issues in three-point bending fracture toughness testing. *ACI Materials journal* 92(5): 483-496.

Salari, M. R., Saeb, S., Willam, K. J., Patchet, S. J. & Carrasco, R. C. 2004. A coupled elastoplastic damage model for geomaterials. *Computer methods in applied mechanics and engineering* 193(27-29): 2625-2643.

Yazdani, S. & Schreyer, H.L. 1988. An anisotropic damage model with dilatation for concrete. *Mechanics of materials* 7(3): 231-244.

Zhao J., Sheng D. & Zhou W. 2005. Shear banding analysis of geomaterials by strain gradient enhanced damage model. *International journal of solids and structures* 42(20): 5335-5355.